



HAL
open science

Blood Compatibility of Multilayered Polyelectrolyte Films Containing Immobilized Gold Nanoparticles

Arnaud Pallotta, Marianne Parent, Igor Clarot, Ming Luo, Vincent Borr, Pan Dan, Véronique Decot, Patrick Menu, Ramia Safar, Olivier Joubert, et al.

► **To cite this version:**

Arnaud Pallotta, Marianne Parent, Igor Clarot, Ming Luo, Vincent Borr, et al.. Blood Compatibility of Multilayered Polyelectrolyte Films Containing Immobilized Gold Nanoparticles. *Particle & Particle Systems Characterization*, 2017, 34 (1), pp.1600184. 10.1002/ppsc.201600184 . hal-01465062

HAL Id: hal-01465062

<https://hal.univ-lorraine.fr/hal-01465062>

Submitted on 16 Mar 2022

HAL is a multi-disciplinary open access archive for the deposit and dissemination of scientific research documents, whether they are published or not. The documents may come from teaching and research institutions in France or abroad, or from public or private research centers.

L'archive ouverte pluridisciplinaire **HAL**, est destinée au dépôt et à la diffusion de documents scientifiques de niveau recherche, publiés ou non, émanant des établissements d'enseignement et de recherche français ou étrangers, des laboratoires publics ou privés.

DOI: 10.1002/ ((please add manuscript number))

Article type: Full paper

Blood Compatibility of Multilayered Polyelectrolyte Films Containing Immobilized Gold Nanoparticles

Arnaud Pallotta✉, *Marianne Parent*✉, *Igor Clarot*, *Ming Luo*, *Vincent Borr*, *Pan Dan*,

Véronique Decot, *Patrick Menu*, *Ramia Safar*, *Olivier Joubert*, *Pierre Leroy*, *Ariane Boudier**

✉ equal contribution to this work

A. Pallotta, Dr. M. Parent, Dr. I. Clarot, Dr. M. Luo, V. Borr, Dr. R. Safar, Dr. O. Joubert, Pr.

P. Leroy, Dr. A. Boudier

Université de Lorraine, CITHEFOR EA 3452, BP 80403, Nancy Cedex, F-54001, France

E-mail: ariane.boudier@univ-lorraine.fr

P. Dan, Dr. V. Decot, Pr. P. Menu

UMR 7365 CNRS Université de Lorraine, Ingénierie Moléculaire et Physiopathologie

Articulaire, Department of Cell and Tissue Engineering, Vectorization, Imaging, Biopôle de

l'Université de Lorraine, Avenue de la forêt de Haye, C.S. 50184, Vandœuvre-lès-Nancy

Cedex F-54505, France

KEYWORDS: gold nanoparticles, layer-by-layer films, nanostructured material, stability, biocompatibility.

ABSTRACT: Surface material functionalization including layer-by-layer (LbL) polyelectrolyte films with incorporated nanoparticles is a growing field with a wide range of biomedical applications: drug reservoirs, medical devices or tissue engineering. In parallel, gold nanoparticles (AuNP) can be **grafted** by drugs and sensitive molecules using simple protocols. This study shows that AuNP behavior is modified when they are entrapped into three partner LbL films in comparison to the colloidal solution. A polycationic (polyallylamine hydrochloride (PAH)) and a polyanionic polymer (polyacrylic acid (PAA)) were used to build films based on 3 cycles ([PAH/AuNP/PAA]₃). To investigate the interaction with biomolecules and cells, three different films were developed changing the outer layer (either PAH or AuNP or PAA) with the same number of AuNP deposit. The best biocompatibility was observed with a polyacrylic acid outer layer. Due to the high capacity of drug grafting on gold nanoparticles, the results seem promising for the development of nanostructured biomedical devices.

1. Introduction

Surface material functionalization is a growing field with a wide range of possible applications. It is usually achieved using various techniques including layer-by-layer (LbL) assemblies.¹ This mean of deposition has attracted an increasing interest since it is a low cost method able to produce reproducible surfaces through simple protocols in order to confer new properties to the material.^[1] Thin films based on LbL assemblies find now applications in electronics, energy, photonics, textile, and paper industry.² In the biomedical domain, they are used as biosensors, drug reservoirs, implantable or not biomedical devices as well as for tissue engineering.^[1,3-5] These last years, micro- or nano-particles were included into LbL assemblies for surface modification to afford high drug loading, stabilization of sensitive molecules (proteins, peptides or nucleic acids) and also the ability to trigger drug release in response to stimuli (pH, temperature, ionic strength, light).^[4,6-8] Among all the existing nanoparticles, a lot of them have already been incorporated into LbL films including polymeric as well as inorganic nanoparticles.^[4,7-8]

Gold nanoparticles (AuNP) are one of the most studied nano-objects and some of them are currently evaluated through clinical trials. They possess the advantages of an easy synthesis, creating well-defined mono-dispersed particles. They can also be **grafted** by drugs and sensitive molecules using simple protocols.^[9] As a result, they can be considered as ideal candidates to functionalize material surface for biomedical purposes. Only few reports related to the development of bioreactive supports focus on their entrapment into LbL films.^[10-13] However, to the best of our knowledge, no report has been published yet on the biocompatibility of assemblies entrapping AuNP for a future application as a drug reservoir inside medical devices. Herein, LbL assemblies including AuNP were prepared and characterized, and their stability and behavior after incubation with biomolecules, plasma-like media, immunocompetent cells and whole blood were studied. Citrate capped AuNP were chosen to be entrapped since they are the most frequently used particles, as they often

represent a first step of synthesis before being grafted.^[14] Moreover, they are interesting in the present study as their gold core is characterized by a residual catalytic activity which induces a poor bio- and cytocompatibility.^[15-16] Thus, after a physicochemical characterization of the prepared LbL films based on polyelectrolytes containing three layers of AuNP, the last component deposited at the surface was varied and the effect of such films on the biological materials was evaluated.

2. Results and discussion

The LbL films, based on polyacrylic acid (PAA), a weak acid ($pK_a = 4.3$) and polyallylamine (PAH), a weak base ($pK_a = 10$), were prepared using the classical dipping protocol.^[17-18] Glassware (cover glass) were successively put into the polycation solution then into the AuNP suspension (as they present a negative zeta potential value)^[15] and finally into the polyanion solution. This cycle was repeated three times. On the contrary to other published works (usually a polyelectrolyte and oppositely charged AuNP)^[10-13], herein, films based on three partners (PAH/AuNP/PAA)_x were developed: indeed, PAA was added in order to improve the biocompatibility of the film, as it will be later explained. Phosphate buffer solution (at the physiological pH and ionic strength) was chosen to solubilize the polyelectrolytes. Its pH allowed the polymers to be mostly under their ionized form. This should create a film characterized by a dense electrostatic binding network,^[5] able to anchor the nano-object and to avoid any release of particles into the external medium (that might induce toxicity)^[19]. Moreover, for a biomedical application, an inert surface is required; therefore we hypothesized that a last negatively charged layer ((PAH/AuNP/PAA)₃), would be less reactive towards biological environment than both AuNP ((PAH/AuNP/PAA)₂-PAH/AuNP) or positively charged ((PAH/AuNP/PAA)₃-PAH) layers.

2.1 Film characterization and stability

After one cycle deposited, a red shift of the plasmon band of AuNP was observed between the colloidal solution and the film (509 ± 1 nm to 544 ± 3 nm, respectively) (**Figure 1A**).

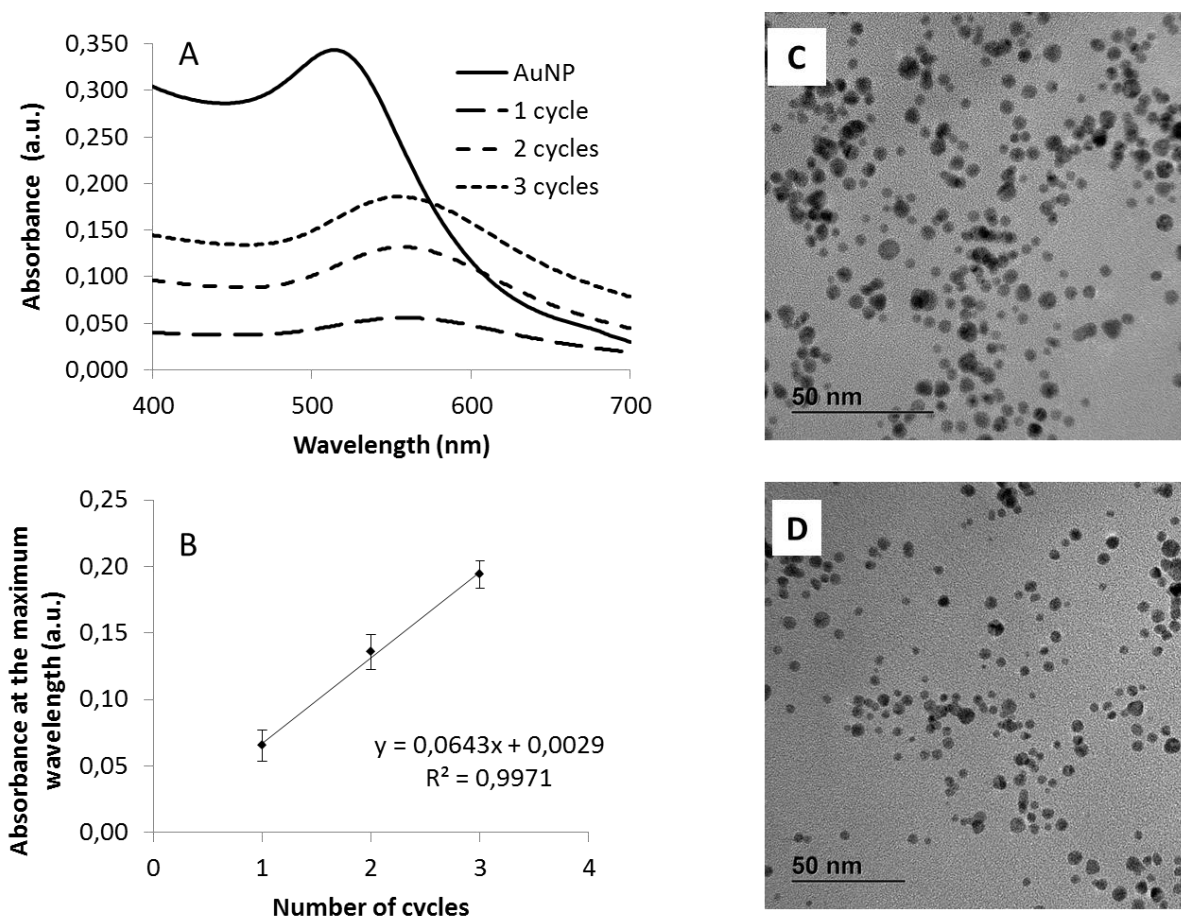


Figure 1. (A) Visible spectra of the colloidal solution and the films and (B) variation of maximal absorbance of the Plasmon band plotted as a function of the number of coating cycles ($n = 9$, for each condition). TEM pictures of (C) AuNP suspension and (D) AuNP entrapped films (PAH/AuNP/PAA)₃.

This phenomenon was already observed and is attributed to differences between nanoparticle environments. Indeed, this is due to modification into the dielectric environment as well as the decrease of inter-particle distance in the film compared to the colloidal solution.^[12-13] However, no significant difference in plasmon band values with the increasing number of cycles was observed. As the absorbance of the nanostructured films was increasing according to a linear profile (**Figure 1B**), the amount of adsorbed AuNP was proportional to the gold layer number. After gold quantification, the amount of gold after three cycles was equal to $2.7 \pm 0.5 \times 10^{12}$ AuNP.cm⁻², which was comparable to other published work.^[10]

Then, transmission electron microscopy (TEM) images (**Figure 1C and D**) were recorded to compare object size and dispersity of colloidal solution and films. The repartition of the particles on the films obtained by TEM pictures (based on a three cycle film *i.e.* (PAH/AuNP/PAA)₃) showed a low density of coverage. This can be explained because of the choice of PAH which presents one basic group per monomer in comparison to previous results reported with polyethylenimine (4 basic groups per unit).^[11] However, the particles looked well-individualized in the films with core diameters of 5.2 ± 0.9 nm (*vs.* 5.3 ± 1.1 nm for the colloidal solution). Therefore, the nanoparticles did not aggregate during film formation.

The stability of the films (PAH/AuNP/PAA)₃ was studied under various conditions. A long term study was led: the films were stored either dried at 4°C or immersed in PBS at 37°C. In both situations, even after one year, neither modification in maximal wavelength nor in absorbance was observed showing an important stability. On the contrary, the colloidal solution was less stable: at 37°C, particle aggregation was noticed after one month for the pure suspension and only after one hour when diluted in PBS. Although the enhanced stability brought by the polyelectrolyte film was already published,^[10] for the first time, a long term storage of such nanostructured films was studied either dried at 4°C or under physiological-like conditions which is of particular importance for a future biomedical application. Moreover, degrading conditions (*i.e.* pH = 1 and 12 or 4 M NaCl) were also tested. Whatever the tested condition, no significant spectral modification was observed (*e.g.* maximal wavelength 548 ± 2 nm, 546 ± 2 nm and 546 ± 3 nm for the acidic, basic and salt conditions, respectively). This result highlighted again an enhanced stability of the nanostructured films compared to the colloidal solution (for which each condition induced a precipitation of the objects), which may be explained by a tightly interconnected network between the three partners. At last, the stability of the films was tested after being exposed to a shear stress during 2 and 6 h mimicking blood flow (1.5 Pa). This value (between 1 and 2 Pa) corresponds

to the physiological value of shear stress in vessels having a diameter of 6 mm (small arteries such as coronaries).^[20] In our experiment, no significant modification in AuNP spectral properties as well as in deposited nanoparticle quantity was observed (**Figure 2**).

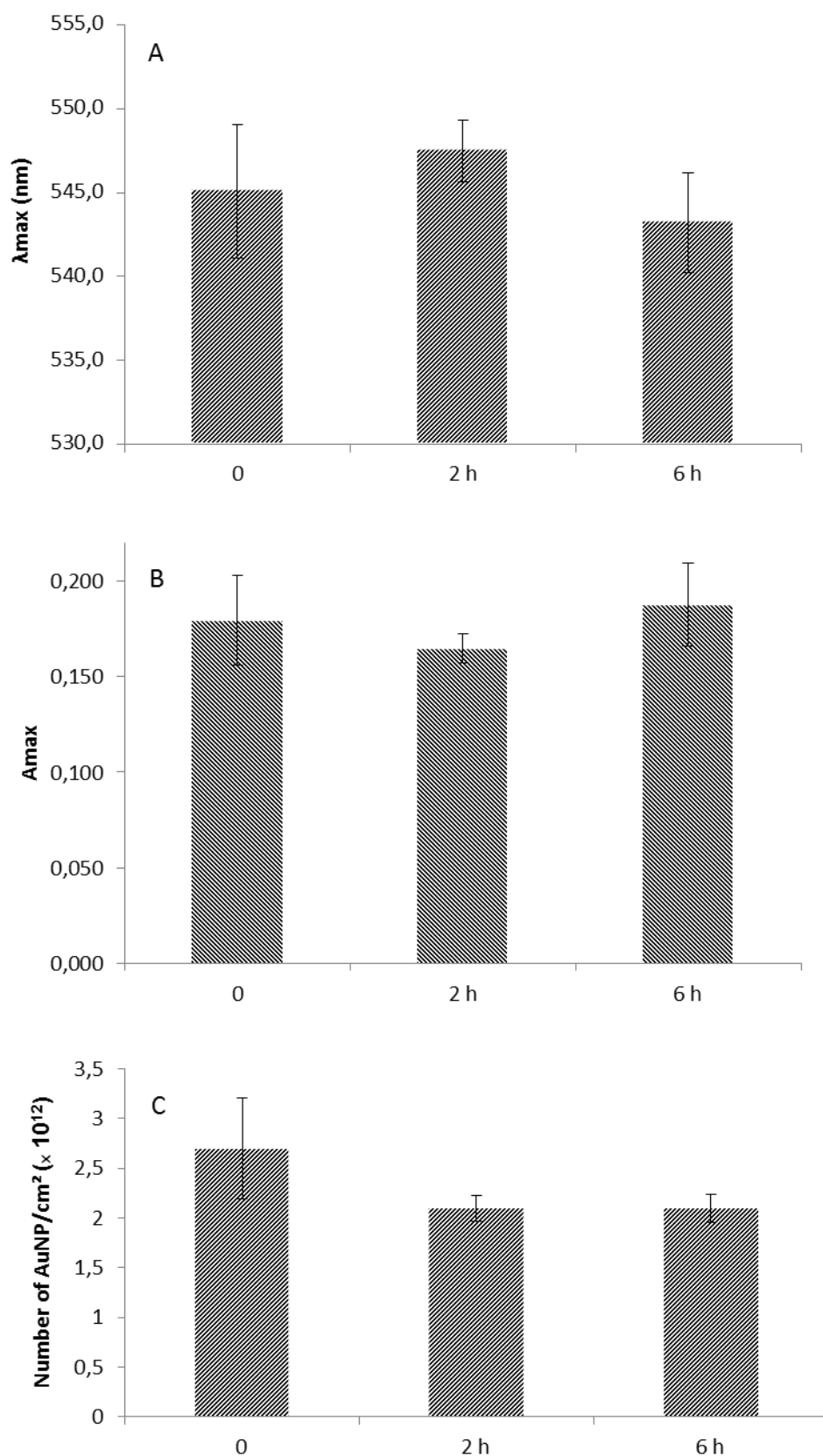


Figure 2. Behavior of films (PAH/AuNP/PAA)₃ after 2 or 6 h exposure to shear stress. The stability was monitored by the spectral properties of the entrapped AuNP (Plasmon band value (A) and absorbance (B)) as well as their quantification (C) (n = 3) Statistical analyses were performed with the Tukey-Kramer test.

2.2 Biocompatibility of nanostructured films

In order to evaluate the biocompatibility of the AuNP-structured films, the last deposited layer (either polycation or AuNP or polyanion) was varied to study its influence on biological materials. Thus, (PAH/AuNP/PAA)₃-PAH, (PAH/AuNP/PAA)₃ and (PAH/AuNP/PAA)₂-PAH/AuNP films were studied according to their surface topography and charge surface using atomic force microscopy (AFM) and capillary zone electrophoresis (CZE), respectively. Analyses in AFM (**Figure 3A, B and C**) revealed that no significant difference in film thickness was noticed whatever the outer layer: 284, 244 and 275 nm for (PAH/AuNP/PAA)₃-PAH, (PAH/AuNP/PAA)₃ and (PAH/AuNP/PAA)₂-PAH/AuNP, respectively.

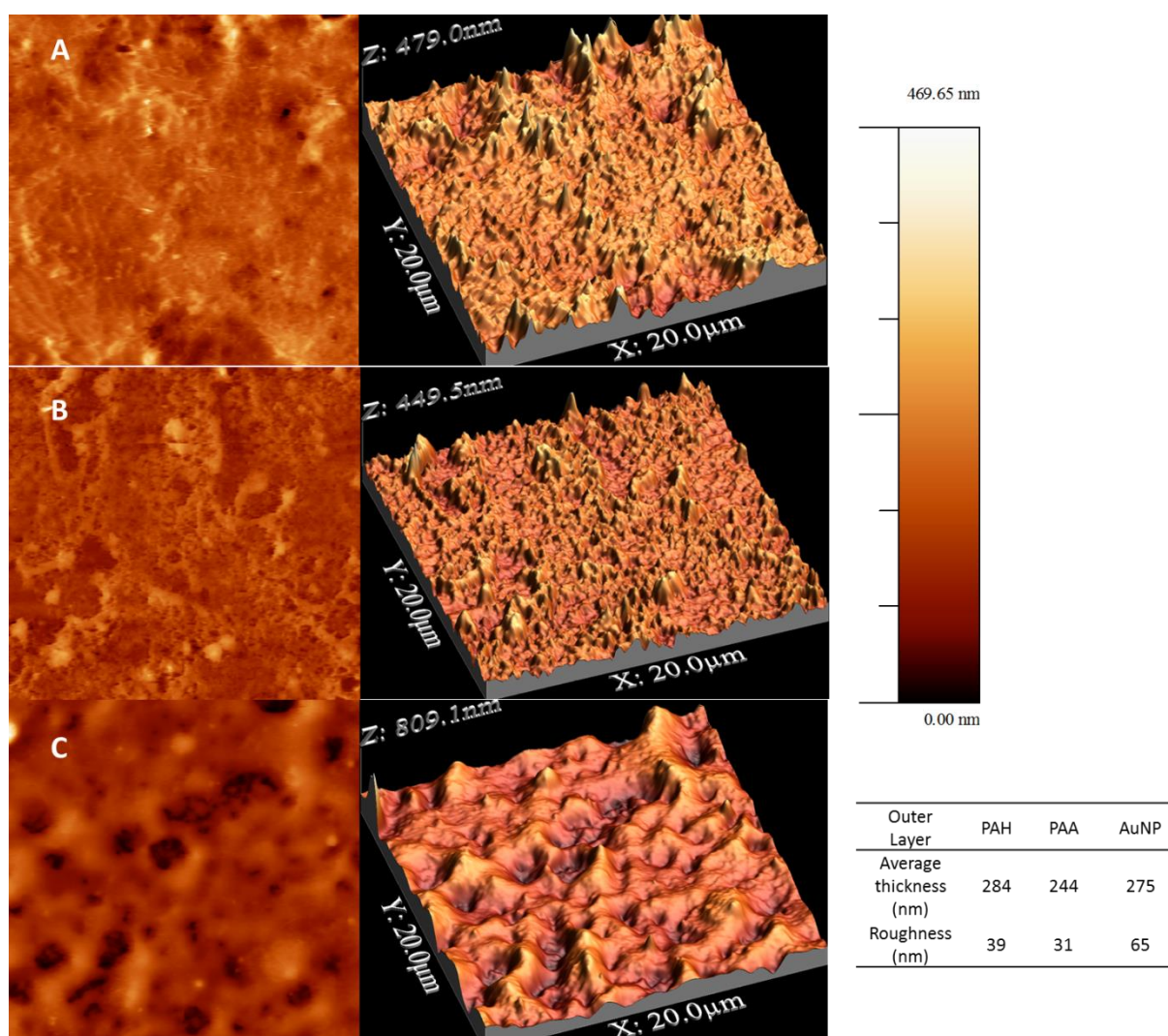


Figure 3.

AFM analyses and surface topography of (A) ((PAH/AuNP/PAA)₃-PAH) (B), (PAH/AuNP/PAA)₃ (C) and ((PAH/AuNP/PAA)₂-PAH/AuNP) films shown in 2 (left) or 3 (right) dimensions.

However, the roughness was more important than previously reported results obtained without AuNP²¹ (few nanometers compared to 39 and 31 nm for (PAH/AuNP/PAA)₃-PAH and (PAH/AuNP/PAA)₃). Lastly, when the outer layer was AuNP, an important roughness (65 nm) was measured and no nanoparticle was observed at the surface of the film even at higher magnification (**Figure 3C**) but rather, a rugged surface was obtained. This fact can be explained by the tight electrostatic interactions developed between PAH and AuNP. Then, CZE which is an interesting separation tool (charged or neutral species migrates inside a fused silica capillary under an applied electric field) was used to assess the surface charge modification of (PAH/AuNP/PAA)₃-PAH, (PAH/AuNP/PAA)₃ and (PAH/AuNP/PAA)₂-PAH/AuNP films. In CZE, the apparent mobilities rely on both charge/mass ratio of the species under investigation and the electroosmotic flow (EOF) resulting from the capillary inner wall charge surface (negatively charged surface due to the ionized silanol groups). For a neutral compound, *i.e.* benzyl alcohol, the observed migration time comes only from the EOF and therefore it is directly in relation to charges of the silica capillary wall surface (sign and magnitude). As an example, a typical electropherogram is shown in **Figure 4A**.

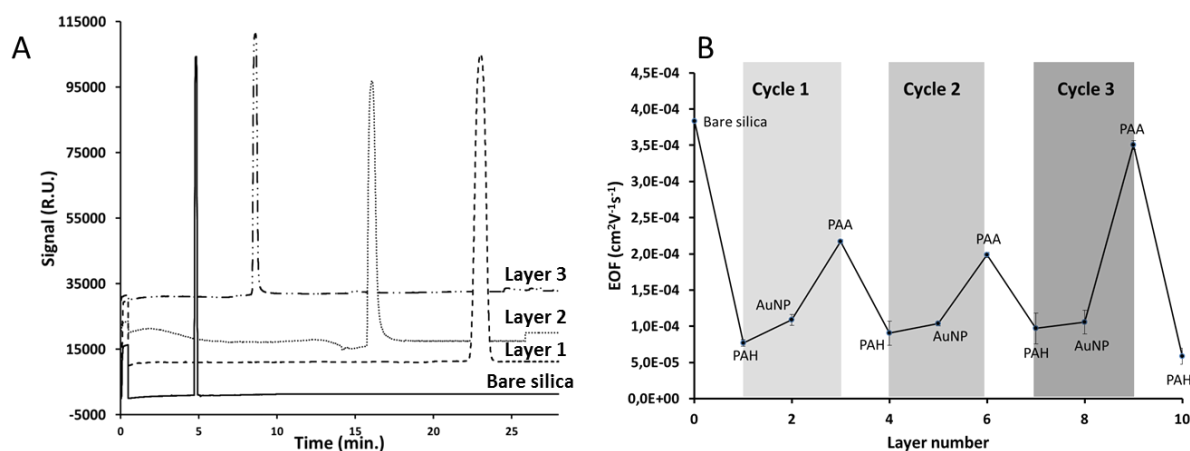


Figure 4.

Electropherograms (A) obtained by CZE for the deposition of the 1st cycle and (B) the calculated EOF as a function of the layer number.

The neutral marker migration time (NMT) as a function of the last deposited layer inside the capillary is monitored. After one PAH layer (layer 1), the NMT drastically increased (from 5 to 24 min) due to positive charges of polycation in tight interaction with bare silica leading to EOF neutralization. Then, the AuNP layer induced a small decrease in NMT (layer 2: NMT = 16 min) due to negative charge deposition. At last, the PAA layer brought a NMT close to bare silica (layer 3: NMT = 9 min) indicating an important anionic surface. The first cycle (PAH/AuNP/PAA) was then repeated twice and EOF obtained for each layer is described in **Figure 4B**. Similar results were measured for each cycle demonstrating the predominant role of the last layer coating. These results showed that (PAH/AuNP/PAA)₃-PAH, (PAH/AuNP/PAA)₃ and (PAH/AuNP/PAA)₂-PAH/AuNP films in which the outer layer was varied were different in terms of surface: roughness and charge which may impact the interaction with biological materials.

In parallel of these physicochemical results, three main biological key-points were assessed: biomolecule and protein adsorption, monocyte activation, and using rat blood: plasma protein interaction and hemolysis of whole blood. First, nanostructured film interaction with biomolecules and proteins is considered as a pivotal parameter that will assess its compatibility.^[21] Therefore, a redox molecule and two proteins presently used at their plasmatic concentrations were selected: reduced glutathione (GSH; 10 μ M) as it easily reacts with AuNP^[9], albumin since it is quantitatively the most important protein in human blood (38 to 48 g.L⁻¹) and fibrinogen (2 to 4 g.L⁻¹) which plays a critical role in platelet adhesion and activation (**Figure 5A, B and C**).^[21]

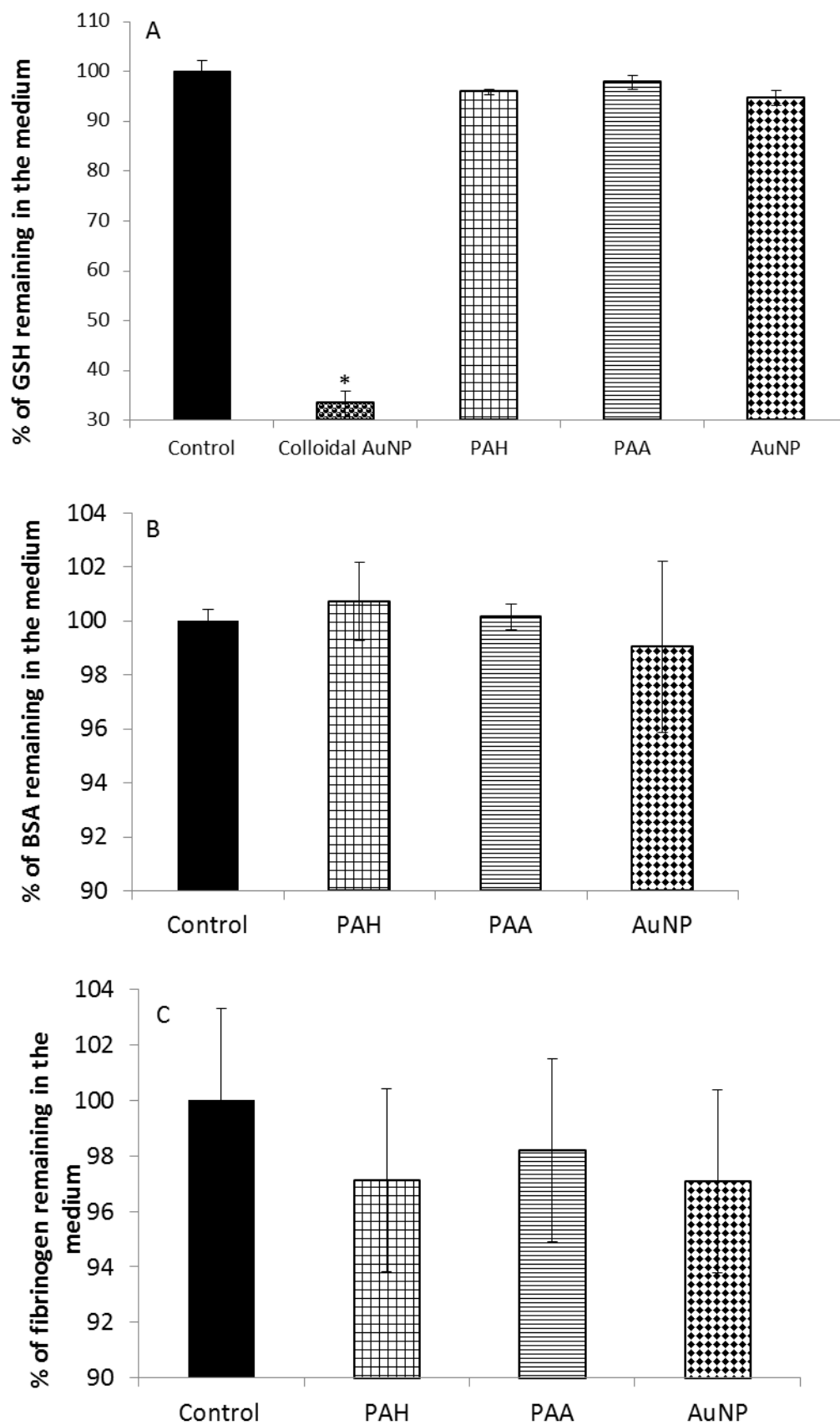


Figure 5.

Biological tests realized onto AuNP either colloidal (5×10^{12} AuNP corresponding to the amount of immobilized NP on the [PAH/AuNP/PAA]₃ film) or entrapped polyelectrolytes films as a function of the outer layer either ((PAH/AuNP/PAA)₃-PAH) or (PAH/AuNP/PAA)₃ or AuNP ((PAH/AuNP/PAA)₂-PAH/AuNP) noted in the figure PAH, PAA and AuNP, respectively or using colloidal AuNP (n = 3). Biomolecule adsorption was realized using reduced glutathione (A) Bovine Serum Albumin (B) and Fibrinogen (C). Controls correspond to the same concentration of glutathione or proteins incubated without film. Statistical analyses were performed with the Tukey-Kramer test (* p < 0.0001 vs control).

For all biomolecules, no significant adsorption was noticed after incubation with the films whatever the last layer. However, a 70 % decrease of initial concentration of GSH was measured after incubation with colloidal AuNP. This highlighted the low AuNP reactivity when immobilized into the films.

Second, monocyte activation was studied after a 48-h incubation of the films with THP-1 cells. Indeed, monocytes are immunocompetent cells able to initiate immune responses as a function of their activation level. Based on two different tests (*i.e.* membrane permeation by Trypan Blue and mitochondrial metabolic activity by WST-1), no toxicity was found (viability superior to 80 %). Then, real-time quantitative Reverse Transcription-Polymerase Chain Reaction (qRT-PCR) analysis was performed to evaluate *NCF1* (Neutrophil Cytosolic Factor 1) and *IL-1 β* (Interleukine-1 β) expression levels. Those genes are considered as classical marker genes of monocyte activation.^[22] Our results (**Figure 6A and B**) showed that the monocyte phenotype was not orientated towards activation since *NCF1* and *IL-1 β* expression was not modified, whatever the last layer, which proved a great cytocompatibility.

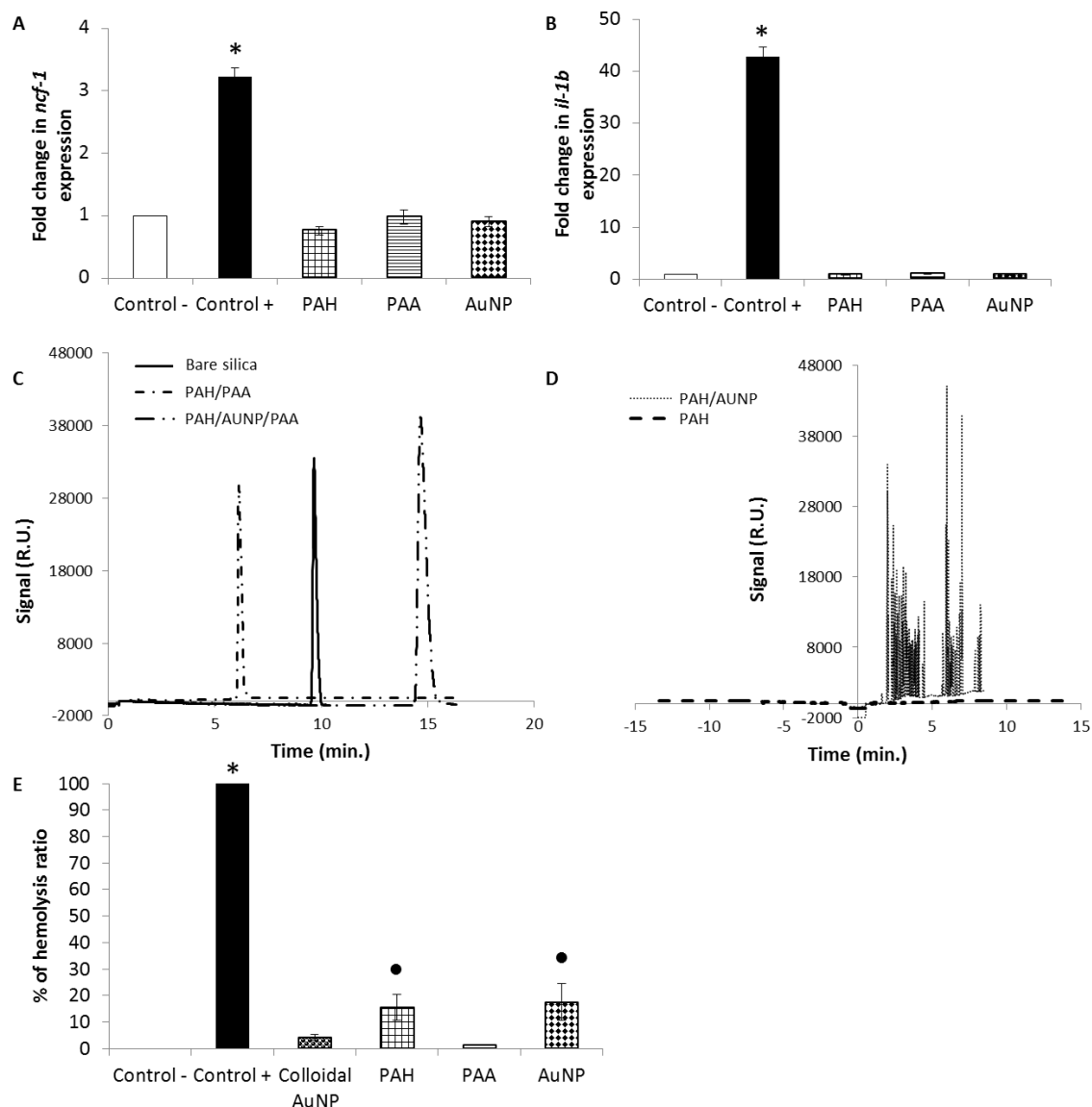


Figure 6.

Biological tests realized onto AuNP either colloidal (5×10^{12} AuNP corresponding to the amount of immobilized NP on the $[\text{PAH}/\text{AuNP}/\text{PAA}]_3$ film) or entrapped polyelectrolytes films as a function of the outer layer either $(\text{PAH}/\text{AuNP}/\text{PAA})_3\text{-PAH}$ or $(\text{PAH}/\text{AuNP}/\text{PAA})_3$ or AuNP $(\text{PAH}/\text{AuNP}/\text{PAA})_2\text{-PAH}/\text{AuNP}$ noted in the figure PAH, PAA and AuNP, respectively or using colloidal AuNP ($n = 3$). Monocyte activation (control -: 10 mL of cell suspension; control +: 10 ng.mL⁻¹ of phorbol 12-myristate 13-acetate added to cells) was checked using real-time qRT-PCR through gene expression rise of *NCF-1* (A) and *IL-1β* (B). Rat plasma interaction with pre-coated capillary was studied after 5 min injection into CZE monitoring the NMT (C and D). Percentage of hemolysis of rat whole blood (E) following the absorbance of hemoglobin after covered slide incubation (control +: 10 mL of water + 0.2 mL of diluted blood; control -: 10 mL of NaCl + 0.2 mL of diluted blood). Statistical analyses were performed with the Tukey-Kramer test (* $p < 0.0001$ vs control- and • $p < 0.0002$ vs control-).

Third, rat plasma was injected into the CZE system with LbL coated capillaries, and after rinsing, the NMT was monitored as a function of the outer deposited layer (PAH or AuNP or

PAA) (**Figure 6C and D**). When comparing the effect of plasma on a bare silica capillary, a protein adsorption inducing a neutralization of the charge surface was noticed; this implied a modification in NMT (10 vs. 5 min when comparing **Figure 6C** and **Figure 4A**) and a decrease in EOF. After PAH and PAH/AuNP coating (**Figure 6D**), the results proved an important surface neutralization (no EOF in normal and reverse polarity) and a lack of stability of the created films (multiple peaks detected), respectively, which may not match the biocompatibility criteria. Using PAA as the outer layer showed the presence of a unique NM peak, revealing a stabilization of the previous layers (PAH/AuNP) (**Figure 6C**). Nevertheless, PAH/AuNP/PAA films proved a more important protein adsorption than PAH/PAA (NMT of *ca.* 15 vs. 6 min, respectively).

At last, films were incubated with rat whole blood to evaluate their capacity to induce hemolysis. In this experiment (**Figure 6E**), the outer layer affected the obtained results. Indeed, only in the case of PAA, the hemocompatibility was proven. The other kinds of films ((PAH/AuNP/PAA)₃-PAH or ((PAH/AuNP/PAA)₂-PAH/AuNP) showed a significant hemolysis. In order to investigate the effect of AuNP, some films based on one layer of PAH, or [PAH/PAA]₁ and [PAH/PAA]₃ were tested according to the same protocol. The results showed no significant hemolysis (2.5 ± 0.3 , 0.5 ± 0.2 and 1.2 ± 0.3 %, respectively) when PAA was placed on the outer layer, emphasizing the best hemocompatibility of films terminated by PAA. Such results were in accordance with the ones obtained on rat plasma. Colloidal AuNP incubated with blood induced a residual hemolysis (4.1 ± 1.1 %) which was, however, not significant.

Taken together, these results highlighted main points. The nature of the outer layer influenced the biocompatibility of the prepared LbL films: when using a polyanion, PAA, better results were obtained with overall good biocompatibility. Indeed, a polycation such as PAH easily interacts with biological materials through electrostatic interactions and AuNP

through redox activity or gold-sulfur bond.^[5,15-16,23] Herein, the outer PAA anionic layer was essential to improve the inertness of the developed three partner-based “sandwich system”.

3. Conclusion

In summary, this study showed that AuNP can be entrapped into such three partners LbL films. No modification of these entrapped particles was highlighted from a physicochemical point of view. Particles also showed an improved stability after long-term storage and also under degrading conditions compared to the colloidal solution. The interaction with biological materials was studied as a function of the outer deposited layer (either PAA or PAH or AuNP). The better cyto/hemocompatibility was obtained using the polyanion as the last depot. This report is the first one to show the behavior and inertness of AuNP immobilized films under biological conditions compared to the colloidal state and the possibility to use them for further biomedical applications. Indeed, these particles can be easily grafted by drugs or biomolecules and then being entrapped into LbL films to act as smart medical devices.

4. Experimental Section

Materials

Poly(allylamine hydrochloride) powder (PAH) and poly(acrylic acid, sodium salt) (PAA) solution 35 % wt in water with average molecular masses of 15,000, penicillin, streptomycin, amphotericin B and Trypan blue solution were purchased from Sigma Aldrich. Solutions of HCl 1 M from Fluka were used for pH adjustments. RPMI medium was purchased from GIBCO (In vitrogen) Dodecyl sulfate sodium salt (SDS) and fetal bovine serum were supplied by Eurobio. 4-[3-(4-Iodophenyl)-2-(4-nitrophenyl)-2H-5-tetrazolio]-1,3-benzene disulfonate (WST-1) was purchased from Roche applied sciences. Phosphate-buffered saline (PBS) solution was prepared as follows: $[\text{Na}_2\text{HPO}_4] = 6.48 \times 10^{-3}$ M, $[\text{KH}_2\text{PO}_4] = 1.47 \times 10^{-3}$ M, $[\text{NaCl}] = 138 \times 10^{-3}$ M, and $[\text{KCl}] = 2.68 \times 10^{-3}$ M, final pH was adjusted to 7.4. All other

reagents were supplied by Sigma Aldrich and were of analytical grade. Ultrapure deionized water ($>18.2 \text{ M}\Omega\cdot\text{cm}$) was used for the preparation of all solutions. Citrate capped gold nanoparticles were synthesized according to^[15].

Animals and blood sampling protocol

All experiments were performed in accordance with the European Community guidelines (2010/63/EU) for the use of experimental animals. Male Wistar rats between 280 and 350 g (Charles River, France) were used in this study. To obtain arterial blood samples, rats were anesthetized (starting 15 min before sample time) with isoflurane (4% in oxygen $2 \text{ L}\cdot\text{min}^{-1}$). After anticoagulation (500 UI of heparin sodium, intravenous administration), a laparotomy was performed to access to the abdominal artery. Blood was obtained directly from the artery through a short PTFE catheter (Intraflon 2, Vygon, France) and collected in Vacutainer (Becton Dickinson, USA) tubes containing heparin lithium.

Plasma was obtained after centrifugation ($10000 \times g$, 15 min, $4 \text{ }^\circ\text{C}$) and keep at $-20 \text{ }^\circ\text{C}$.

Film preparation

The glass substrates used for the deposition ($24 \times 36 \times 0.145 \text{ mm}$, Menzel-Glaser) were cleaned with SDS 0.1 M at $100 \text{ }^\circ\text{C}$ for 15 min, followed by extensive rinsing with water. They were then immersed in HCl 0.1 M at $100 \text{ }^\circ\text{C}$ for 15 min, extensively rinsed and finally dried.

Polyelectrolyte solutions (0.1 M according to monomers molecular masses) were prepared freshly before each experiment in PBS. Addition of HCl 1 M in the PAA solution was required to adjust pH to 7.4. The fabrication of AuNPs/polymer multilayer film was carried out as follows. A pre-treated glass slide was dipped in the solution of PAH for 10 min, and then rinsed with two successive baths of PBS (2 min and 1 min, respectively). Subsequently, the slide was immersed in the AuNPs suspension for 10 min, then rinsed as previously described, and finally dipped in the PAA solution for 10 min, rinsed and at the end dried. The AuNPs-incorporating polymer multilayer film was obtained by the repetition of this simple three-step process in a cyclic fashion leading to $(\text{PAH}/\text{AuNP}/\text{PAA})_3$. In some experiments, the

last bath was either PAH ((PAH/AuNP/PAA)₃-PAH) or AuNP ((PAH/AuNP/PAA)₂-PAH/AuNP).

Film characterization

Absorbance spectra (400-700 nm) of the coated slides (*vs.* an uncoated pre-cleaned slide) were recorded on a UV-1800 apparatus (Shimadzu). For stability studies, slides were kept dried at 4 ± 4 °C or in an incubator at 37 ± 1 °C in 10 mL of PBS filtered on 0.22 μ m. At predetermined time, absorbance spectrum of each slide was recorded. As controls, 10 mL of AuNP (pure and diluted 1/3 in PBS) were kept in the same conditions and their spectra recorded against PBS. Experiments were run in triplicate.

Additional stability studies were performed on slides *vs.* pH 1 and 12 (using HCl 1 M and NaOH 1 M and NaCl 4 M). Slides were dipped in the solution for 15 min and an absorbance spectrum was recorded.

For TEM, the films were deposited on carbon covered copper grids (Agar) using the previous protocol but decreasing the incubation time from 10 to 3 min and a last washing of 1 min in water. Then, images were recorded using a Philips CM20 instrument with a LaB6 cathode operating at 200 kV. The average diameter of the gold core was calculated for each AuNP sample by counting *ca.* 200 individual particles from the TEM images. For AFM, films were prepared on glassware slides and immersed into PBS for analysis using a MFP3D-BIO instrument (Asylum Research Technology, Atomic Force F & E GmbH, Mannheim, Germany). Gold quantification was performed according to^[24] with some slight modifications. Three slides were crushed with a glass rod and carefully transferred into a vial and 1 mL of an oxidant solution (HCl 1 M, NaCl 2.6 M and Br₂ 0.035 M) was added. After an incubation of 20 min under stirring at 20°C and 1 h at 60°C, gold was quantified using the protocol of Tournebize et al.^[24]

For shear stress experiments, a parallel-chamber flow system (Masterflex, USA) was used. Briefly, shear stress experiments were carried out at 37°C in a 5% CO₂ incubator, 7.5 × 3.8 cm glass coverslips coated with (PAH/AuNP/PAA)₃ were placed on the top of the flow chamber allowing fluid flux to pass through the coated surface. The shear stress was gradually increased to 1.5 Pa and lasted for 2 or 6 h.^[25] Glass coverslips were then disassembled for the stability test.

Capillary zone electrophoresis

All experiments were performed on a Beckman P/ACE 5500 model (Beckman, Fullerton, USA) equipped with a UV detector set at $\lambda = 200$ nm in normal polarity mode, anodic injection (negative times indicate a reverse polarity). Capillary temperature was controlled by coolant at 25.0 °C. An untreated fused-silica capillary, 50 μ m internal diameter with a total length of 37 cm (effective length: 30 cm) was employed. The neutral marker benzyl alcohol (0.1 mg.mL⁻¹ in background electrolyte, BGE) was injected in the hydrodynamic mode (10 s under pressure) at 10 kV. The experimental set-up, data acquisition, and processing were governed using Beckman P/ACE Station software. The BGE was ten-fold diluted PBS. For the first experiment, the capillary was rinsed with 1.0 M sodium hydroxide (20 min) and ultrapure water (20 min). Each injection was realized in triplicate, results were indicated as a mean and residual standard deviations were always lower than 3.0 %. Polyelectrolyte solutions used to coat the capillary were those described in the film preparation section. Rapidly, for each layer, the capillary was first filled with the coating solution (PAH or AuNP or PAA) at 20 psi for 3 min and rinsed with the same solution at 0.5 psi (low pressure mode) for 30 min. Between each layer, benzyl alcohol was injected three times and before each injection, the capillary was successively rinsed with ultrapure water (2 min) and BGE (3 min). The EOF mobility was determined using the migration time (NMT) of the EOF marker and Equation 1:

$$EOF = \frac{L \times l}{NMT \times V} \quad (1)$$

where L and l are the total and the apparent lengths of the capillary (length to detection) and V the applied voltage.

In a second set of experiments, plasma samples were diluted in BGE 20 % and injected during 5 min. under a pressure of 20 psi. Then, BGE was used to rinse the capillary and the surface charge was evaluated by three injection of the NM. The capillary was rinsed with NaOH 1.0 M (20 min) and H₂O (20 min) to recover the initial silanol surface.

Reactivity with reduced glutathione

In a water bath at 37 ± 1 °C, slides were equilibrated 1h in PBS then incubated for 2 h in 10 mL of GSH 10 μ M in PBS. The remaining GSH concentration in the dipping solution was determined using Ellman's method. Briefly, 200 μ L of 5,5'-dithio-bis(2-nitrobenzoic) acid solution (1 mM in Na₂HPO₄ 0.1 M and EDTA 2 mM buffer, pH 7.5) were added to 1 mL of sample. The resulting mixture was incubated for 10 min at room temperature protected from light, before its absorbance was measured at 412 nm. Calibration curve was obtained with a standard GSH solution (3.25 mM in HCl 0.1 M) diluted in the Na₂HPO₄/EDTA buffer, in the range 3.25 – 32.5 μ M. As a control, colloidal AuNP were diluted in PBS to obtain a final amount of 5×10^{12} NP and the resulting suspension was centrifuged at $40\,000 \times g$ at 4 ± 1 °C for 30 min before performing Ellman's reaction.

Reactivity with proteins

To evaluate the adsorption of proteins, slides were equilibrated for 1 h at 37 ± 1 °C in PBS, then incubated for 2 h in a solution of bovine serum albumin (BSA, 40 g.L⁻¹ in PBS) or

fibrinogen (2 g.L^{-1} in PBS). After experiment, slides were rinsed carefully with PBS and dried. Remaining BSA and fibrinogen in the dipping solution were evaluated by spectrofluorimetry (278/340 nm, excitation and emission bandwidth 5 nm, response 0.5 s, sensitivity low, linearity range 50 to $1000 \mu\text{g.mL}^{-1}$, spectrofluorimeter FP-8300, Jasco).

Interaction with monocytes

Each experiment was done with 3 independent biological replicates. Human THP-1 monocytes (ATCC® TIB-202™, Manassas, VA, USA) were grown according to ATCC recommendations in order to obtain three independent cultures. Ten milliliters of cell suspension were put into polypropylene tubes at $150 \times 10^3 \text{ cells.mL}^{-1}$. After one day, slides were soaked in the tubes. A negative control (10 mL of cell suspension) was realized. As a positive control, cells were exposed to 10 ng.mL^{-1} of phorbol 12-myristate 13-acetate. Cell viability was assessed after 24 and 48 h exposure performing Trypan Blue and WST-1 methods. Variation of expression of NCF1, IL-1 β was followed. After 24 h of exposure, cells were washed twice with sterile PBS and total RNA was extracted by TRIzol® Reagent (Invitrogen, La Jolla, CA) following manufacturer's protocol. Real-time quantitative Reverse Transcription-Polymerase Chain Reaction analyses were performed according the conditions of our previous work.^[22]

Interaction with blood

Hemolysis ratio of the coated cover glasses was measured using a method described previously with slight modifications.²⁶ Briefly, the cover glasses were pre-incubated for 1 h in 10 mL of sterile NaCl 0.9 % (B-Braun) into flat-bottom bottles kept at $37 \pm 1 \text{ }^\circ\text{C}$ in a shaking water bath. Whole arterial blood from a male Wistar rat was diluted (2 mL of blood for 2.5 mL of NaCl 0.9 %) ($n = 3$). Immediately, 0.2 mL of diluted blood was added into each bottle containing 10 mL of sterile NaCl 0.9 % or water for the positive control. Cover glasses were

soaked in the blood solution for another 1 h. Finally, solutions were centrifuged at $1,000 \times g$ for 5 min and absorbance of the supernatant was measured at 576 nm. Colloidal AuNP were diluted into blood to obtain a final amount of 5×10^{12} NP, and the resulting suspension was centrifuged at $40\,000 \times g$ at $4 \pm 1^\circ\text{C}$ for 30 min before absorbance measurements. Hemolysis ratio (HR) was obtained by Equation 2:

$$HR = 100 * \frac{(AS - AN)}{(AP - AN)} \quad (2)$$

where AS is the absorbance of sample supernatant, AP and AN are the absorbance of positive (10 mL of water + 0.2 mL of diluted blood) and negative controls (10 mL of NaCl + 0.2 mL of diluted blood), respectively.

Supporting Information

This work was financially supported by *Université de Lorraine* (project 2015, supervisor Dr A. Boudier, project AAP-002-100)

Acknowledgements

The authors want to thank Pr. R. Schneider, Pr. D. Rouxel, and Dr G. Francius for AuNP synthesis, TEM and AFM facilities

Received: ((will be filled in by the editorial staff))

Revised: ((will be filled in by the editorial staff))

Published online: ((will be filled in by the editorial staff))

References

- [1] R. R. Costa, J. F. Mano, *Chem. Soc. Rev.* **2014**, *43*, 3453.
- [2] J.-F. Chapel, J.-F. Berret, *Curr. Opin. Colloid. Interface Sci.* **2012**, *17*, 97.
- [3] K. Sato, S. Takahashi, J. Anzai, *Anal. Sci.* **2012**, *28*, 929.
- [4] S. Pavlukhina, S. Sukhishvili, *Adv. Drug Deliv. Rev.* **2011**, *63*, 822.
- [5] Z. Tang, Y. Wang, P. Podsiadlo, N. A. Kotov, *Adv. Mater.* **2006**, *18*, 3203.

- [6] X. Liu, P. K. Chu, C. Ding, *Mater. Sci. Eng. R Rep.* **2010**, *70*, 275.
- [7] S. Srivastava, N. A. Kotov, *Acc. Chem. Res.* **2008**, *41*, 1831.
- [8] H. Takahashi, D. Letourneur, D. W. Grainger, *Biomacromolecules* **2007**, *8*, 3281.
- [9] B. Duncan, C. Kim, V. M. Rotello, *J Controlled Release* **2010**, *148*, 122.
- [10] D. M. Dotzauer, J. Dai, L. Sun, M. L. Bruening, *Nano Lett.* **2006**, *6*, 2268.
- [11] T. Placido, E. Fanizza, P. Cosma, M. Striccoli, M. L. Curri, R. Comparelli R, A. Agostiano, *Langmuir* **2014**, *30*, 2608.
- [12] Z. M. Qi, I. Honma, M. Ichihara, H. S. Zhou, *Adv. Funct. Mater.* **2006**, *16*, 377.
- [13] M. M. Ottakam Thotiyil, H. Basit, J. A. Sanchez, C. Goyer, L. Coche-Guerente, P. Dumy, S. Sampath, P. Labbé, J. C. Moutet, *J. Colloid. Interface Sci.* **2012**, *383*, 130.
- [14] E. C. Dreaden, A. M. Alkilany, X. Huang, C. J. Murphy, M. A. El-Sayed, *Chem. Soc. Rev.* **2012**, *41*, 2740.
- [15] J. Tournebize, A. Boudier, O. Joubert, H. Eidi, G. Bartosz, P. Maincent, P. Leroy, A. Sapin-Minet, *Int. J. Pharm.* **2012**, *438*, 107.
- [16] J. Tournebize, A. Boudier, A. Sapin-Minet, P. Maincent, P. Leroy, R. Schneider, *ACS Appl. Mater. Interfaces* **2012**, *4*, 5790.
- [17] A. I. Petrov, A. A. Antipov, G. B. Sukhorukov, *Macromolecules* **2003**, *36*, 10079.
- [18] G. Decher, *Science* **1997**, *277*, 1232.
- [19] N. Khlebtsov, L. Dykman, *Chem. Soc. Rev.* **2011**, *40*, 1647.
- [20] D. Giddens, C. Zarins, S. Glagov, *J. Biomech. Eng.-Trans. Asme.* **1993**, *115*, 588.
- [21] H. - W.Chien, S. -F. Tan, K. -L. Wei, W. -B. Tsai, *Colloids Surf. B-Biointerfaces* **2011**, *88*, 297.
- [22] C. Ronzani, R. Safar, R. Diab, J. Chevrier, J. Paoli, M. A. Abdel-Wahhab, A. Le Faou, B. H. Rihn, O. Joubert, *Cell. Biol. Toxicol.* **2014**, *30*, 137.
- [23] J. Tournebize, A. Sapin-Minet, G. Bartosz, P. Leroy, A. Boudier, *Talanta* **2013**, *116*, 753.

[24] J. Tournebize, A. Sapin-Minet, R. Schneider, A. Boudier, P. Maincent, P. Leroy, *Talanta* **2011**, *83*, 1780.

[25] C. Gaucher-Di Stasio, E. Paternotte, C. Prin-Mathieu, B. J. Reeder, G. Poitevin, P. Labrude, J. F. Stoltz, C. E. Cooper, P. Menu, *Biomaterials* **2009**, *30*, 445.

[26] X. Ye, X. Hu, H. Wang, J. Liu, Q. Zhao, *Acta Biomater.* **2012**, *8*, 1057.

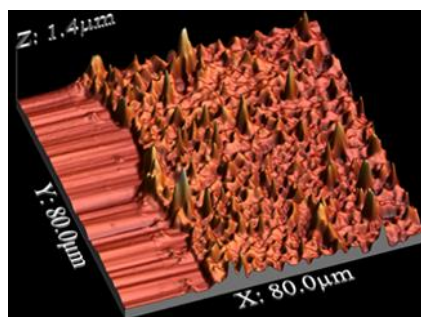
Gold nanoparticle stability is enhanced when they are entrapped into three partner layer-by-layer polyelectrolyte films compared to the colloidal solution. The best biocompatibility regarding various biological materials is observed when a polyacrylic acid is present at the outer layer. Due to the high capacity of drug grafting on gold nanoparticles, the results seem promising for the development of nanostructured biomedical devices.

Keyword: gold nanoparticles, layer-by-layer films, nanostructured material, stability, biocompatibility

Arnaud Pallotta[✉], Marianne Parent[✉], Igor Clarot, Ming Luo, Vincent Borr, Pan Dan,

Véronique Decot, Patrick Menu, Ramia Safar, Olivier Joubert, Pierre Leroy, Ariane Boudier*

Blood Compatibility of Multilayered Polyelectrolyte Films Containing Immobilized Gold Nanoparticles



ToC figure